Assessment of thermal coagulation in *ex-vivo* tissues using Raman spectroscopy

Matthew Rodrigues
Ryerson University
Department of Physics
350 Victoria Street
Toronto, ON, M5B 2K3 Canada

Robert A. Weersink
Ryerson University
Department of Physics
350 Victoria Street
Toronto, ON, M5B 2K3 Canada
    and
Ontario Cancer Institute
University Health Network
610 University Avenue
Toronto, ON, M5G 2M9 Canada

William M. Whelan
University of Prince Edward Island
Department of Physics
Charlottetown, PE, C1A 4P3 Canada
    and
Atlantic Veterinary College
Department of Biomedical Sciences
Charlottetown, PE, C1A 4P3 Canada

Abstract. Raman spectroscopy is used to study the effects of heating on specific molecular bonds present in albumen-based coagulation phantoms and *ex-vivo* tissues. Thermal coagulation is induced by submerging albumen-based phantoms in a 75°C water bath to achieve target temperatures of 45, 55, 65, and 75°C. Laser photocoagulation is performed on *ex-vivo* bovine muscle samples, yielding induced temperatures between 46 and 90°C, as reported by implanted microthermocouples. All phantoms and tissue samples are cooled to room temperature, and Raman spectra are acquired at the microthermocouple locations. Shifts in major Raman bands are observed with laser heating in bovine muscle, specifically from the amide-1 α-helix group ($\sim$1655 cm^{-1}), the CH$_2$/CH$_3$ group ($\sim$1446 cm^{-1}), the Cα-H stretch group ($\sim$1312 cm^{-1}), and the CN stretch group ($\sim$1121cm^{-1}). Raman bands at 1334 cm^{-1} (tryptophan), 1317 cm^{-1} [ν(Cα-H)], and 1655 cm^{-1} (amide-1 α-helix) also show a decrease in intensity following heating. The results suggest that Raman band locations and relative intensities are affected by thermal denaturation of proteins, and hence, may be a useful tool for monitoring the onset and progression of coagulation during thermal therapies. © *2010 Society of Photo-Optical Instrumentation Engineers*. [DOI: 10.1117/1.3512231]

1 Introduction

Raman spectroscopy is an inelastic scattering process in which incident photons transfer energy to (Stokes) or gain energy from (anti-Stokes) molecules within a sample. At room temperature, Stokes Raman is the dominant process, where molecules simultaneously absorb energy from an incident photon and emit a photon of lower energy. The difference in energy corresponds to vibrational modes of the interrogated molecule. Each wavelength shift is chemical specific, and therefore bands in a Raman spectrum can be assigned to particular chemical structures within a sample.[1] Raman spectroscopic techniques for biomedical applications have seen significant advancement over the past decade, with improvements in portability of equipment and fiber-optic-based excitation and collection, which allows for interstitial applications.[2] Raman spectroscopy has also been shown to provide information about the structure of molecular constituents in tissues,[3,4] and has the ability to distinguish between normal and cancerous tissues under certain conditions. Raman spectroscopy has seen widespread use in cancer research, including the detection and diagnosis of breast cancer,[5,6] basal cell carcinoma,[7,8] as well as bladder and prostate cancer.[9,10]

Raman spectroscopy has also been applied to study the effects of heating on proteins and enzymes. Protein denaturation is defined as a conformational change in the secondary and tertiary structures of the native protein without cleavage of peptide bonds within the amino acid sequence. Partial or complete as well as reversible or irreversible-denaturation can be observed due to factors such as temperature, pH changes, and pressure.[11] Torreggiani et al. employed Raman spectroscopy to obtain an accurate evaluation of the heat-induced conformational changes of lysozyme before and after sulfoxide addition.[12] Fourier transform (FT)-Raman spectroscopy was used to show that heated samples of solid unprocessed, spray-dried, and crystallized trypsin showed some perturbations of their secondary structures and some biological activity when heated below their denaturation temperatures, and were insoluble with complete loss of biological activity when heated above their denaturation temperatures.[13] The influence of sugars on the mechanism of thermal denaturation was also examined using Raman spectroscopy, and it was determined that the thermal stability of the hydrogen bond network in water contributes to the stabilization of the tertiary structure, inhibiting the first stage of denaturation.[14] FT Raman spectroscopy was used to study changes in the conformation of heated solid lactate dehydrogenase (LDH) and trypsinprotein samples, showing that heating dry proteins above their denaturation temperature perturbed the secondary structure. Raman spectroscopy has also been applied to investigate a number of effects and interactions on human and bovine serum albumin proteins.[15,16] A shift in the CH$_2$CH$_3$ deformation band near 1450 cm^{-1} and the amide-1 α-helix band near 1660 cm^{-1}, as well as an increase in the Raman intensity in

Address all correspondence to: William M. Whelan, Atlantic Veterinary College, Department of Biomedical Sciences, Charlottetown, PE, C1A 4P3 Canada. Tel: 902-566-0419; Fax: 902-566-0483. E-mail: wwhelan@upei.ca.
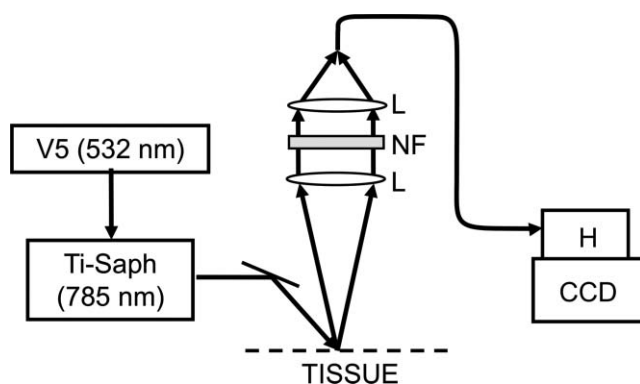
Fig. 1 Schematic of the Raman system including autofocusing lenses (L), notch filter (NF), axial transmissive imaging spectrograph (H), and liquid nitrogen cooled charge-coupled device (CCD).

the amide-3 β-sheet structure (1240 cm^{-1}), have been observed in egg albumin heated at 90°C for 30 min.[17]

In this work, we investigate whether Raman spectroscopy can differentiate between native and coagulated tissues by detecting changes in tissue protein structure following heating.

2 Materials and Methods

2.1 Raman System

An overview of the Raman system employed in this work is depicted in Fig. 1. The excitation source was a titanium-sapphire (Ti-saph) laser operating at 785 nm pumped by a Nd:YVO$_4$ solid-state laser (V5) with intracavity doubling operating at 532 nm. The output power of the Ti-Saph at the sample surface was 100 mW. After the incident light interacts with the sample, the remitted light from the surface of the sample enters the first portion of the collection optics, consisting of two autofocusing lenses (L) (Nikon 85 and 50 mm) and a notch filter (NF). The light is then focused onto a fiber optic bundle consisting of 43 fibers (200 μm, NA of 0.28, CeramOptec Industries, Incorporated, East Longmeadow, Massachusetts). The bundle is connected to an axial transmissive imaging spectrograph (H) (Holospec f/1.8i, Kaiser Optical Systems Incorporated, Ann Arbor, Michigan) with the fibers aligned along the entrance slit of the spectrograph. The grating had a spectral resolution of 12 cm^{-1} when the 200-μm slit was used with 785-nm excitation. Light detection is made with a front illuminated, liquid nitrogen cooled charge-coupled device (CCD) (Photometrics Limited, Tucson, Arizona) coupled to the exit port of the spectrograph. All Raman spectra were collected with an integration time of 15 s, repeated for 15 cycles, for a total collection time of 225 s per spectrum, giving an acceptable signal-to-noise ratio. Two spectra were acquired for each sample, resulting in a dataset for each sample consisting of 60 spectra. The responsivity of the system was corrected according to the procedure outlined by Shim and Wilson,[18] and the fluorescence background was subtracted using the adaptive minmax method recently developed by Cao et al. and adapted appropriately for use with the collected raw data.[19]

2.2 Tissue Equivalent Albumen Phantoms

Albumen-based phantoms that coagulate on heating were fabricated based on a recipe published by Iizuka, Sherar,

and Vitkin.[20] Albumen protein is comprised mainly of water (88.1%), globular proteins (10.2%), and lipids (0.05%), and is commercially available as dehydrated egg white powder. The phantom used consisted of chicken egg albumen (Crude, grade 2, Sigma, Saint Louis, Missouri), bacteriological agar (Oxoid, Hampshire, England), and Naphthol Green dye (Sigma, Saint Louis, Missouri). The solid phantoms were constructed by combining the agar-dye solution, heated to 85°C, and the albumen stock solution, heated to 40°C. This mixture was then poured into cylindrical molds with a diameter of 6 cm and height of 3 cm, and cooled to room temperature. Thermal coagulation was performed by submerging each phantom in a water bath maintained at 75°C until the target temperature was reached, as reported by a microthermocouple placed at the center of the phantom. The phantom was then immediately removed, placed into a cold water bath at approximately 22°C, and allowed to cool. Performing the coagulation in this manner mimics thermal therapy treatments, in that once a defined target temperature is reached, heating ceases and the tissue is allowed to cool. Each phantom was heated to a target temperature of 45, 55, 65, or 75°C. Each phantom was then cut in half and Raman spectra were acquired at the center of each sample, identified by the indentation in the phantom made by the microthermocouple. This ensured that Raman spectra were collected at the exact region where the temperature was recorded during heating.

2.3 Laser Photocoagulation of Bovine Muscle

Bovine muscle was selected for laser photocoagulation based on previous experimental results and data available in the literature on the Raman spectra for muscle.[3,21] Photocoagulation was performed using an 805 nm diode laser (Diomed Incorporated, Andover, Massachusetts) coupled to a 400-μm core optical fiber with a 20-mm cylindrical diffusing tip. The laser fiber was placed at the center of a tissue slab. Microthermocouples were placed at 2, 5, and 10 mm from the center of the diffusing tip. A second tissue slab was placed on top, followed by a weight to ensure good tissue coupling. The input laser power was set to 7 W and the irradiation was terminated when a temperature of 90°C was recorded by the thermocouple positioned 2 mm from the source fiber. The tissue slab was then allowed to cool to room temperature ($\sim$22°C).

3 Results and Discussion

3.1 Tissue Equivalent Albumen Phantoms

Raman spectra, normalized to the band at 1000 cm^{-1} for each phantom experiment, are shown in Fig. 2. When normalizing Raman spectra, it is essential to choose a band that is not sensitive to the conformational changes to ensure that any observed band shifts are identifiable. The 1000 cm^{-1} band does not change in shape or position with heating, suggesting that it is not sensitive to any conformational changes. Raman peak intensity increases with final temperature achieved, most notably in the major bands representing albumen protein, such as phenylalanine C=C symmetric stretch (1002 cm^{-1}), CH$_2$,CH$_3$ deformation (1463 cm^{-1}), and the amide-1 β-sheet (1663 cm^{-1}).[22–25] Several features, such as the phenylalanine C=C symmetric stretch
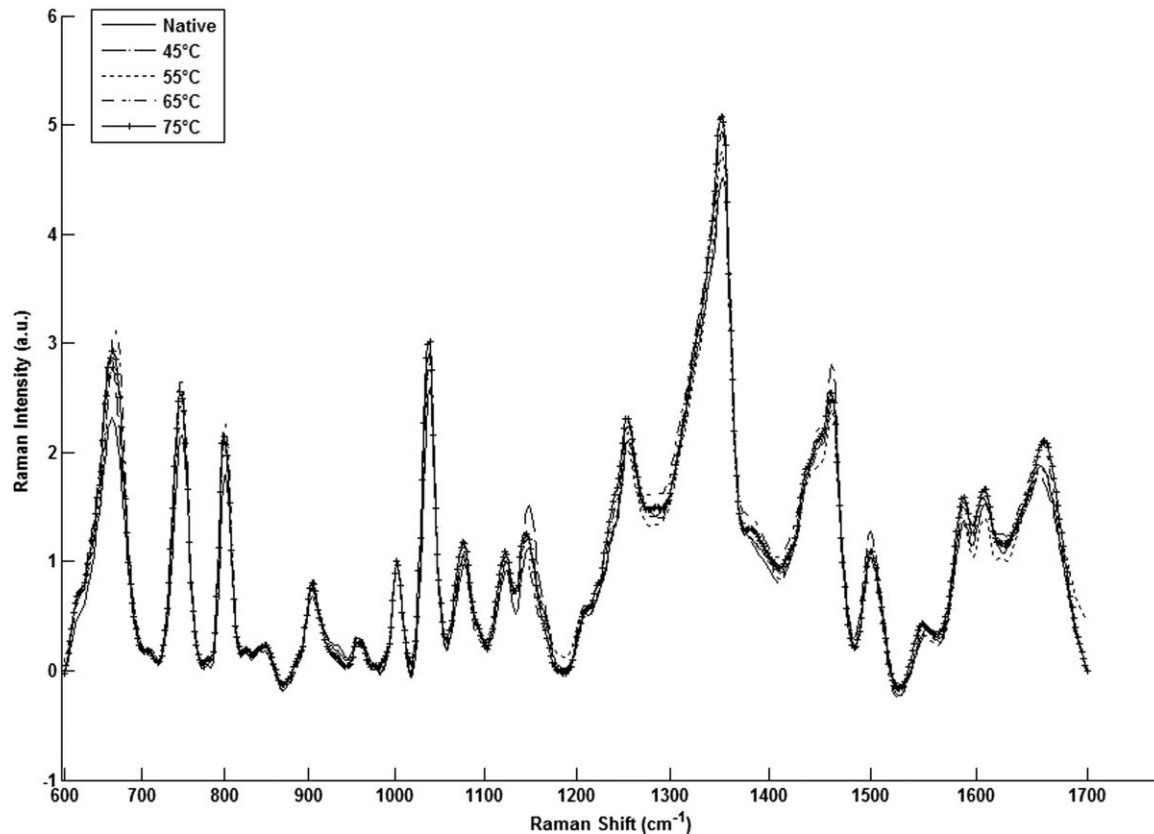
Fig. 2 Raman spectra of albumen-based phantoms at room temperature, and heated to temperatures of 45, 55, 65, and 75°C. Spectra are individually normalized to the intensity at 1000 cm^{-1}.

(1002 cm^{-1}) and CH$_2$/CH$_3$ deformation (1463 cm^{-1}), remain at the same frequency regardless of final temperature achieved. However, there is a shift in the amide-1 β-sheet from 1658 cm^{-1} in the native state to 1663 cm^{-1} in the 75°C coagulated state, which may be a result of changes in vibrational modes resulting from coagulation. This shift is in agreement with Ngarize, Adams, and Howell, who observed a 3 cm^{-1} shift in the amide-1 band in egg albumen heated to 90°C.[23] The absence of shifts in other major bands (phenylalanine C=C at $\sim$1002 cm^{-1} and CH$_2$/CH$_3$ deformation at $\sim$1463 cm^{-1}) may be indicative of the more stable secondary protein structure being less susceptible to the effects of coagulation. The denaturation temperature of two major components of albumen (ovalbumin and conalbumin) have been determined to be 84.5 and 61.0°C, respectively.[26] The shift in the amide-1 band may be an indication of the secondary structure of conalbumin being affected by heating to 65 and 75°C, in addition to tertiary structure alterations due to thermal coagulation. These results suggest that the increased signal is primarily due to increased optical scattering associated with protein coagulation. It has been reported that the scattering coefficient (μ_s) of albumen-based phantoms can increase by a factor of $\sim$17 after 40 min of heating in a 70°C water bath.[27] These results are consistent with other reports of coagulation-induced increases in optical scattering and diffuse reflectance in tissues.[28,29] It is believed that these increases in scattering result from denaturation and hyalinization (a glassy appearance) of collagen and other proteins. The coagulation-induced increase in scattering can increase the photon flux from the sample surface, similar to the increase in diffuse reflectance that occurs with increased scattering.[29]

3.2 *Laser Photocoagulation of Bovine Muscle*

A thermal lesion created in bovine muscle is shown in Fig. 3. The locations of the laser fiber and three thermocouples are clearly visible by indentations in the tissue. Fig. 4 shows the corresponding Raman spectra at 2, 5, and 10 mm, where temperatures reached 90.0, 57.0, and 46.6°C, respectively. The relative intensities of all spectra have been normalized to the band at 1000 cm^{-1}. Several Raman bands are easily identifiable, specifically those near 935 cm^{-1} [ν(CC) skeletal α-helix], 952 cm^{-1} (CH$_2$ bending), 1000 cm^{-1} [Phenylalanine ν(C=C)], 1074 cm^{-1} and 1123 cm^{-1} [ν(CN)], 1317 cm^{-1} [ν(Cα-H)], 1334 cm^{-1} (tryptophan), 1448 cm^{-1} [δ(CH$_2$/CH$_3$)], and 1655 cm^{-1} (amide-1 α-helix).[3,22,24,25] The Raman spectra acquired at 2 mm from the laser fiber (90°C) show a number of notable band shifts. Specifically, there are band shifts in the [ν(CN)] group from 1121 to 1123 cm^{-1}, the [ν(Cα-H)] group from 1312 to 1317 cm^{-1}, and the [δ(CH$_2$/CH$_3$)] group from 1446 to 1448 cm^{-1}. The largest shift was observed in the amide-1 α-helix, which shifted from 1648 cm^{-1} in the native state to 1655 cm^{-1} in the 90°C coagulated state, similar to the results observed in the albumen phantoms. The bands at 952 and 1000 cm^{-1} do not undergo a Raman shift at temperatures up to 90°C, which may indicate that the secondary and tertiary structures of these particular components of the collagen protein are
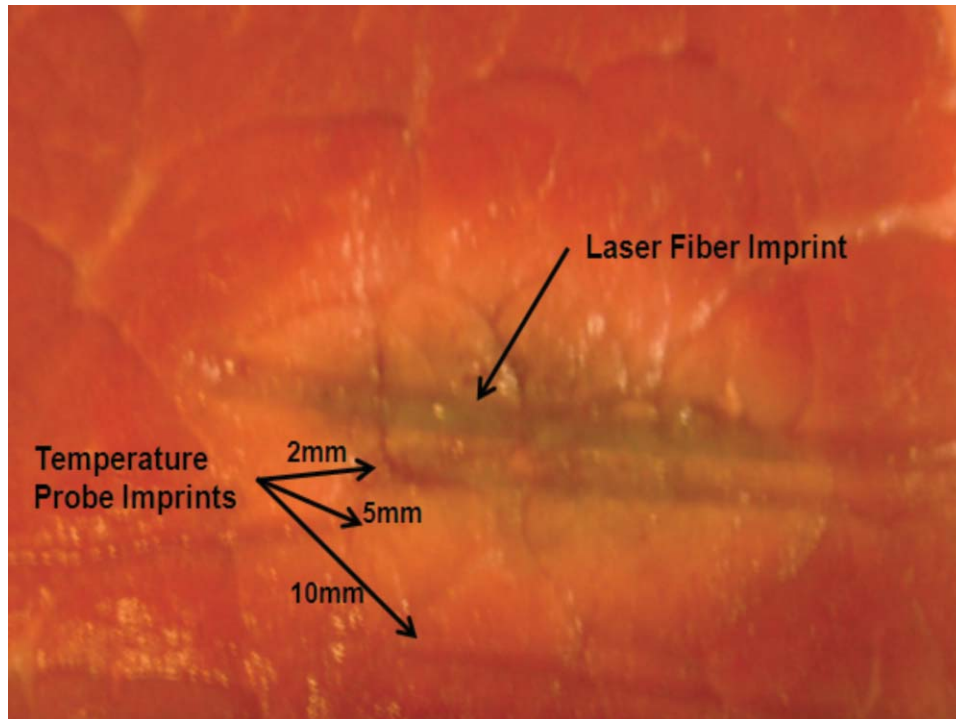
Fig. 3 Thermal lesion created in bovine muscle samples heated with an 805-nm laser operating at 7 W. Indentations by the laser fiber and three thermocouples are indicated.
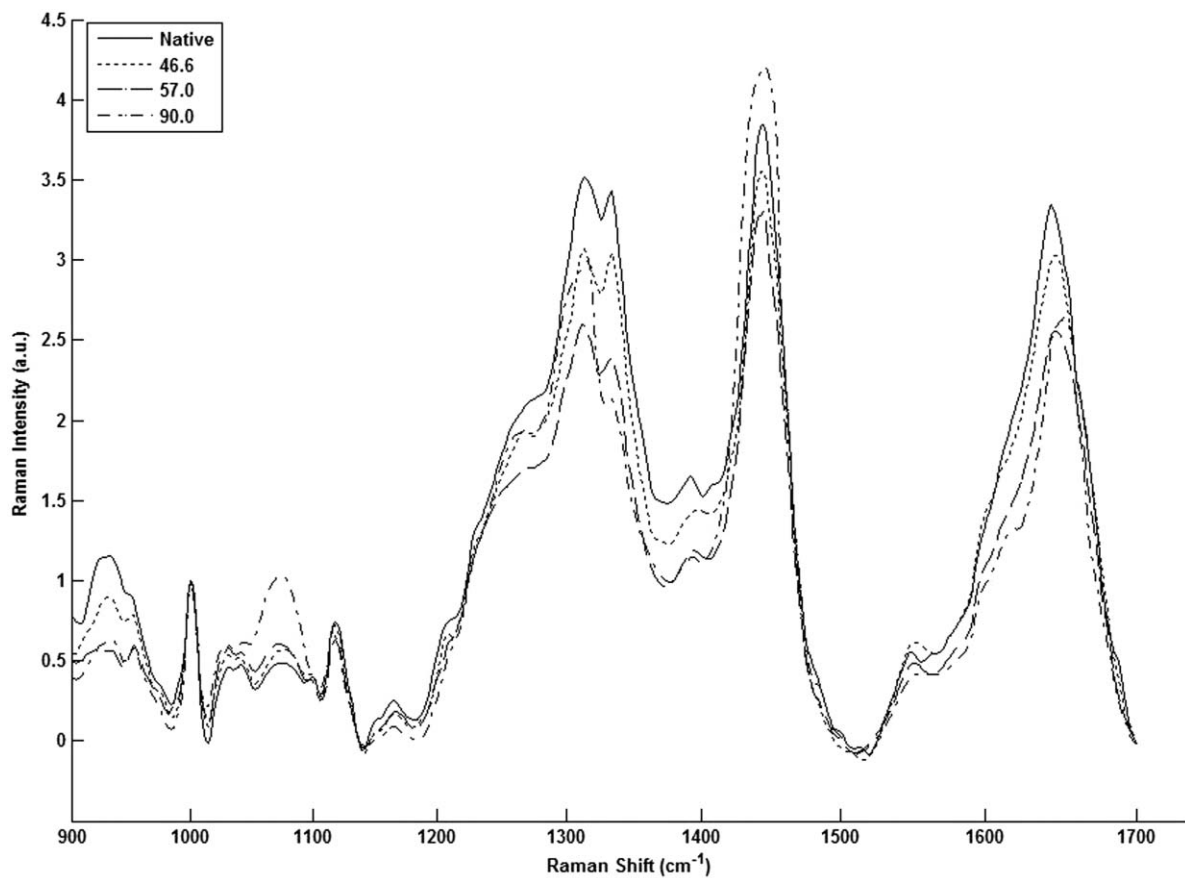

Fig. 4 Raman spectra of bovine muscle in the native state and heated by laser photocoagulation to maximum temperatures of 90.0, 57.0, and 46.6°C, measured at 2, 5, and 10 mm from the laser fiber, respectively. Spectra are individually normalized to the intensity at 1000 cm^{-1}.

stable and less susceptible to effects of heating. Alternatively, the absence of shifts in these bands may indicate only that they arise from vibrations that are not interested in the structural variations by heating. This result is consistent with Dong et al., who noted that the Raman band near 1000 cm^{-1} [phenylalanine ν(C=C)] did not undergo a shift with heating to 80°C.[24]

Unlike Raman measurements on the phantoms, the relative intensities of the Raman bands in muscle varied with temperature, which affected the overall spectral shape. A change is observed in the slope of the shoulder leading up to the band at (Cα-H) 1317 cm^{-1}. In the native and 46.6°C states, this shoulder gradually rises toward the peak; however, in the 57.0°C state, the shoulder becomes steeper, and in the 90.0°C spectrum, the shoulder rises sharply from ~1230 to ~1270 cm^{-1} and then plateaus. A second sharp rise can be seen at ~1290 cm^{-1} toward the peak at 1313 cm^{-1}. Another point of note is the significant reduction in relative intensity of the tryptophan band at 1334 cm^{-1} on heating to 90°C. As the neighboring bands increase in intensity, this band nearly disappears from the Raman spectrum. This intensity decrease may be explained by the degradation of tryptophan's large indole side chain due to heating. Protein-bound tryptophan residues degrade on heating to temperatures over 100°C.[30,31] Further, ~46 to 55% of tryptophan residues in a lactose-tryptophan mixture were lost with heating at 155°C for 2 min.[32] Therefore, heating the bovine muscle sample to 90°C may cause a reduction in the protein-bound tryptophan residues thus reducing the number of Raman interactions that can cause the tryptophan band at 1334 cm^{-1} to be reduced in intensity. Reduction in the intensity of the amide-1 α-helix at 1655 cm^{-1} may be due to dehydration of this component as water is removed from the protein via heating, causing a reduction in the number of Raman interactions. Further, significant changes in the shoulders leading up to both bands {1317 cm^{-1} [ν(Cα-H)] and 1655 cm^{-1} (amide-1 α-helix} are observed. Disruption of secondary structures is typically detected through changes of the band shape, which in turn leads to a frequency shift of the vibrational mode. It may be this phenomenon that results in the reduction in intensity on heating to 57.0°C. However, on heating to 90.0°C, the intensity in both bands increases. This increase is interesting and may represent a transition in the tissue response to heating at higher temperatures. For example, tissue browning is observed near the 2-mm thermocouple (Fig. 3). It is also reported that the biological effects of heating on tissues begins as enzyme inactivation and mitochondrial injury and transitions at approximately 60°C to protein denaturation, membrane rupture, pyknosis, and hyperchromasia.[33] Moreover, such a transition from decreasing intensity to increasing intensity may prove to be a relevant metric for thermal therapy monitoring.

4 Conclusions

Raman spectra acquired before and after heating of tissue equivalent albumen phantoms reveal changes in intensity that increase with maximum temperature achieved. This may be attributed to the increase in the scattering coefficient as tissue proteins within the phantom undergo thermal coagulation, which causes an increase in the remitted photon density from the sample surface. While the secondary structures of some protein constituents such as the phenylalanine band at 1000 cm^{-1} remain unchanged re-

gardless of the increases in temperature, a number of other bands are altered in *ex-vivo* bovine tissue due to thermal denaturation. This is evident by the shifts in major Raman bands such as those arising from the amide-1 group (~1655 cm^{-1}), the CH$_2$/CH$_3$ group (~1446 cm^{-1}), the Cα-H stretch group (~1312 cm^{-1}), and the CN stretch group (~1121cm^{-1}), which may be useful in determining tissue damage due to coagulation during thermal therapies and other procedures.

Additionally, Raman spectra acquired after heating of bovine muscle reveal similar intensity increases in the majority of major Raman bands as well as similar Raman shifts as seen in the albumen phantoms. However, bands at 1334 cm^{-1} (tryptophan), 1317 cm^{-1} [ν(Cα-H)] and 1655 cm^{-1} (amide-1 α-helix) show a decrease in Raman intensity on heating. This may suggest that heating causes degradation in the components of these protein constituents, resulting in fewer Raman interactions and a decrease in Raman intensity. Also, where the amide-1 α-helix is concerned, the decrease in intensity may also be attributed to dehydration of this component as water is removed from the protein through heating. Hence, the Raman spectra provide direct quantitative information on the coagulation state of the tissue. If this is indeed the case, it may be possible to exploit this effect and focus on these bands as possible biochemical markers for monitoring thermal therapies online and in real time. Other optically based measurements of coagulation that rely on measuring the relative change in intensity or radiance are actually indirect measures of the change in tissue scattering resulting from structural changes in the tissue. They are also sensitive to changes in equipment alignment during the procedure. With Raman spectroscopy, the tissue changes are expressed as relative spectral changes between bands, and are therefore much less sensitive to alignment effects.

The results presented in this work suggest that Raman band locations and relative intensities are affected by thermal denaturation of proteins and degradation of protein constituents. It is also possible that measurements of band shifts and intensity changes may be a useful tool in monitoring the onset and progression of coagulation during thermal therapies.

References

1. A. Mahadevan-Jansen and R. R. Richards-Kortum, "Raman spectroscopy for the detection of cancers and precancers," *J. Biomed. Opt.* **1**(1), 31–70 (1996).
2. S. Naito, Y. K. Min, K. Sugata, O. Osanai, T. Kitahara, H. Hiruma, and H. Hamaguchi, "In vivo measurement of human dermis by 1064 nm-excited fiber Raman spectroscopy," *Skin Res. Technol.* **14**(1), 18–25 (2008).
3. B. W. D. De Jong, T. C. B. Schut, K. P. Wolffenbuttel, J. M. Nijman, D. J. Kok, and G. J. Puppels, "Identification of bladder wall layers by Raman spectroscopy." *J. Urol.* **168**(4), 1771–1778 (2002).
4. I. Notingher, S. Verrier, H. Romanska, A. E. Bishop, J. M. Polak, and L. L. Hench, "In situ characterisation of living cells by Raman spectroscopy," *Spectroscopy* **16**(2), 43–51 (2002).

5. S. K. Majumder, M. D. Keller, F. I. Boulos, M. C. Kelley, and A. Mahadevan-Jansen, "Comparison of autofluorescence, diffuse reflectance, and Raman spectroscopy for breast tissue discrimination," *J. Biomed. Opt.* **13**(5), 054009 (2008).

6. R. Manoharan, K. Shafer, L. Perelman, J. Wu, K. Chen, G. Deinum, M. Fitzmaurice, J. Myles, J. Crowe, R. R. Dasari, and M. S. Feld, "Raman spectroscopy and fluorescence photon migration for breast cancer diagnosis and imaging," *Photochem. Photobiol.* **67**(1), 15–22 (1998).

7. A. Nijssen, K. Maquelin, L. F. Santos, P. J. Caspers, T. B. Schut, J. C. den Hollander, M. H. A. Neumann, and G. J. Puppels, "Discriminating basal cell carcinoma from perilesional skin using high wave-number Raman spectroscopy," *J. Biomed. Opt.* **12**(3), 034004 (2007).

8. M. A. Short, H. Lui, D. McLean, H. Zeng, A. Alajlan, and X. K. Chen, "Changes in nuclei and peritumoral collagen within nodular basal cell carcinomas via confocal micro-Raman spectroscopy," *J. Biomed. Opt.* **11**(3), 034004 (2006).

9. M. K. Tollefson, J. S. Magera, T. Sebo, J. Cohen, A. Drauch, J. Maier, and I. Frank, "Raman molecular imaging of prostate cancer: Can Raman spectroscopy be used to predict patient outcome after radical prostatectomy?" *J. Urol.* **179**(4), 224–225 (2008).

10. P. Crow, A. Molckovsky, N. Stone, J. Uff, B. Wilson, and L. M. Wongkeesong, "Assessment of fiberoptic near-infrared Raman spectroscopy for diagnosis of bladder and prostate cancer," *Urol.* **65**(6), 1126–1130 (2005).

11. D. Whitford, *Proteins: Structure and Function*, Wiley, New York (2005).

12. A. Torreggiani, M. Di Foggia, I. Manco, A. De Maio, S. A. Markarian, and S. Bonora, "Effect of sulfoxides on the thermal denaturation of hen lysozyme: a calorimetric and Raman study," *J. Mole. Structure* **891**(1–3), 115–122 (2008).

13. R. T. Forbes, B. W. Barry, and A. A. Elkordy, "Preparation and characterisation of spraydried and crystallised trypsin: FT-Raman study to detect protein denaturation after thermal stress," *Euro. J. Pharmaceut. Sci.* **30**(3-4), 315–323 (2007).

14. A. Hedoux, J. F. Willart, R. Ionov, F. Affouard, Y. Guinet, L. Paccou, A. Lerbret, and M. Descamps, "Analysis of sugar bioprotective mechanisms on the thermal denaturation of lysozyme from Raman scattering and differential scanning calorimetry investigations," *J. Phys. Chem. B* **110**(45), 22886–22893 (2006).

15. I. M. Vlasova, and A. M. Saletsky, "Raman spectroscopy in investigations of mechanism of binding of human serum albumin to molecular probe fluorescein," *Laser Phys. Lett.* **5**(5), 384–389 (2008).

16. I. M. Vlasova, D. V. Polyansky, and A. M. Saletsky, "Investigation of mechanism of binding of molecular probe eosin to human serum albumin by Raman spectroscopy method," *Laser Phys. Lett.* **4**(5), 390–394 (2007).

17. S. Ngarize, A. Adams, and N. K. Howell, "Studies on egg albumen and whey protein interactions by FT-Raman spectroscopy and rheology," *Food Hydrocoll.* **18**(1), 49–59 (2004).

18. M. G. Shim and B. C. Wilson, "Development of an in vivo Raman spectroscopic system for diagnostic applications," *J. Raman Spectrosc.* **28**(2–3), 131–142 (1997).

19. A. Cao, A. K. Pandya, G. K. Serhatkulu, R. E. Weber, H. Dai, J. S. Thakur, V. M. Naik, R. Naik, G. W. Auner, R. Rabah, and D. C. Freeman, "A robust method for automated background subtraction of tissue fluorescence," *J. Raman Spectrosc.* **38**(9), 1199–1205 (2007).

20. M. N. Iizuka, M. D. Sherar, and I. A. Vitkin, "Optical phantom materials for near infrared laser photocoagulation studies," *Lasers Surg. Med.* **25**(2), 159–169 (1999).

21. M. Rodrigues, R. Weersink, and W. Whelan, "Raman spectroscopy: potential for detecting tissue coagulation during laser therapy," in *Biomed. Opt. OSA Tech. Digest* (CD), paper BTuF46, Optical Society of America (2008).

22. H. Gremlich and B. Yan, *Infrared and Raman Spectroscopy of Biological Materials*, Marcel Dekker Inc., New York (2001).

23. S. Ngarize, A. Adams, and N. Howell, "A comparative study of heat and high pressure induced gels of whey and egg albumen proteins and their binary mixtures," *Food Hydrocoll.* **19**(6), 984–996 (2005).

24. R. X. Dong, X. L. Yan, X. F. Pang, and S. G. Liu, "Temperature-dependent Raman spectra of collagen and DNA," *Spectrochimica Acta Part A-Molec. Biomole. Spectrosc.* **60**(3), 557–561 (2004).

25. A.J.P Alix, G. Pedanou, and M. Berjot, "Fast determination of the quantitative secondary structure of proteins by using some parameters of the raman amide-1 band," *J. Mole. Structure* **174**, 159–164 (1988).

26. J. Goetz, and P. Koehler, "Study of the thermal denaturation of selected proteins of whey and egg by low resolution NMR," *Lwt-Food Sci Technol.* **38**(5), 501–512 (2005).

27. R. F. Castelino, W. M. Whelan, and M. C. Kolios, "Photoacoustic detection of tissue coagulation in albumen-based phantoms," *Proc. SPIE* **6856**, 685626 (2008).

28. W. C. Lin, C. Buttemere, and A. Mahadevan-Jansen, "Effect of thermal damage on the in vitro optical and fluorescence characteristics of liver tissues," *IEEE J. Sel. Topics Quantum Electron.* **9**(2), 162–170 (2003).

29. D. J. Parekh, L. W. Chiang, and S. D. Herrell, "In vivo assessment of radio frequency induced thermal damage of kidney using optical spectroscopy," *J. Uro.* **176**(4), 1626–1630 (2006).

30. J. C. Cuq, and J. C. Cheftel, "Tryptophan degradation during heat-treatments. 1. The degradation of free-tryptophan," *Food Chem.* **12**(1), 1–14 (1983).

31. J. C. Cuq, M. Vie, and J. C. Cheftel, "Tryptophan degradation during heat-treatments. 2. Degradation of protein-bound tryptophan," *Food Chem.* **12**(2), 73–88 (1983).

32. V. Moreaux and I. BirlouezAragon, "Degradation of tryptophan in heated betalactoglobulin-lactose mixtures is associated with intense Maillard reaction," *J. Agricultural Food Chem.* **45**(5), 1905–1910 (1997).

33. M. Nikfarjam, V. Muralidharan, and C. Christophi, "Mechanisms of focal heat destruction of liver tumours," *J. Surg. Res.* **127**, 208–223 (2005).